2012

Dependence of magnetoelectric properties on sintering temperature for nano-SiC-doped MgB2/Fe wires made by combined in situ/ex situ process

Wenxian Li
University of Wollongong, wenxian@uow.edu.au

Rong Zeng
University of Wollongong, rzeng@uow.edu.au

Jiazhao Wang
University of Wollongong, jiazhao@uow.edu.au

Y Li
Shanghai University China

S. X. Dou
University of Wollongong, shi@uow.edu.au

Recommended Citation

Li, Wenxian; Zeng, Rong; Wang, Jiazhao; Li, Y; and Dou, S. X.: Dependence of magnetoelectric properties on sintering temperature for nano-SiC-doped MgB2/Fe wires made by combined in situ/ex situ process 2012, 07E135-1-07E135-3.
https://ro.uow.edu.au/engpapers/2934

AIP | Journal of Applied Physics

Dependence of magnetoelectric properties on sintering temperature for nano-SiC-doped MgB2/Fe wires made by combined in situ/ex situ process

W. X. Li, R. Zeng, J. L. Wang, Y. Li, and S. X. Dou

Citation: J. Appl. Phys. **111**, 07E135 (2012); doi: 10.1063/1.3677660
View online: http://dx.doi.org/10.1063/1.3677660
View Table of Contents: http://jap.aip.org/resource/1/JAPIAU/v111/i7
Published by the American Institute of Physics.

Dependence of magnetoelectric properties on sintering temperature for nano-SiC-doped MgB_2/Fe wires made by combined *in situ/ex situ* process

W. X. Li,[1,2] R. Zeng,[1] J. L. Wang,[2] Y. Li,[2] and S. X. Dou[1,a)]
[1]*Institute for Superconducting and Electronic Materials, University of Wollongong, Northfields Avenue, Wollongong, NSW 2522, Australia*
[2]*School of Materials Science and Engineering, Shanghai University, Shanghai 200072, People's Republic of China*

(Presented 3 November 2011; received 22 September 2011; accepted 16 November 2011; published online 7 March 2012)

Very fine nano-SiC particles (<15 nm) were doped into a MgB_2 superconductor. The influence of self-field supercurrent on the high-field performance of the nano-SiC-doped MgB_2/Fe wires is discussed based on comparison of the critical current densities of the *in situ* processed nano-SiC-doped MgB_2 wires and those of the nano-SiC-doped MgB_2/Fe wires processed by the combination of *in situ/ex situ* methods. © *2012 American Institute of Physics*. [doi:10.1063/1.3677660]

The critical current density (J_c) of MgB_2 superconductors has been advanced through many different kinds of dopants or additives,[1] especially different carbon sources.[2–8] J_c values as high as 1×10^4 A cm^{-2} at $\sim$12.5 T, 4.2 K have been reported for 10 wt % SiC-doped *in situ* wires. However, the self-field critical current density values, $J_c(0)$, of these samples are much lower than those of samples made by hybrid physical–chemical vapor deposition (HPCVD),[9,10] 3.5×10^7 A/cm^2 at 4.2 K and 1.6×10^8 A/cm^2 at 2 K. The depairing current density, J_d, is $\sim 8.7 \times 10^8$ A/cm^2 for pure MgB_2.[9] The connectivity is poor in *in situ* MgB_2 samples because the *in situ* technique involves a solid–liquid reaction process with considerable shrinkage as a result of the high theoretical density of MgB_2 compared to the initial mixture of Mg and B.[11–13] It is critically important to discover how to make a high-density sample to obtain high $J_c(0)$ and then introduce strong flux-pinning force to keep J_c dropping as slowly as possible with increasing magnetic field. High-pressure sintering, especially hot isostatic pressing (HIP) treatment is used in making high-density bulks and wires.[14] Cold high-pressure densification (CHPD) is also effective in improving the density to as high as 73% in wires.[12,13] However, the equipment for the high-pressure processes is quite complicated, and the sample densities are still lower than needed for practical application. The *ex situ* technique is promising for making high J_c MgB_2 superconductors.[13,15] The problem with the *ex situ* technique is the low-quality connections between the MgB_2 grains. In this work, a mixed *in situ/ex situ* technique was employed to develop nano-SiC-doped MgB_2 wires with high connectivity and strong flux-pinning force to increase both the low- and high-field J_c properties. The SiC particle size is another critical issue for introducing strong flux-pinning forces into MgB_2. The size of SiC used in this work is smaller than the sizes used in previous research, and the J_c dependence on sintering temperature also shows a very different trend.[2,12,16,17]

The powder-in-tube (PIT) process was employed to make practical MgB_2 wires from a ball-milled mixture of Mg (99%), B (99%, amorphous), and SiC (<15 nm). A part of the mixture was made into MgB_2/Fe wires with a diameter of 1.4 mm, which were sintered in high-purity Ar at temperatures of 750, 850, 950, and 1050 °C for 30 min as standard *in situ* samples, which were marked as 750in, 850in, 950in, and 1050in, respectively. The other part of the mixture was sintered at 650 °C for 30 min in pure argon flow and then ball-milled to yield precursor MgB_2 powder. Then *in situ/ex situ* combined MgB_2/Fe wires were made by the PIT method using this precursor powder and a mixed powder in a 1:3 ratio. All the green wires were annealed in high-purity Ar at temperatures of 750, 850, 950, and 1050 °C for 30 min, yielding samples that were marked as 750inex, 850inex, 950inex, and 1050inex, respectively.

According to the indexed XRD patterns as shown in Fig. 1, all samples show quite high purity of MgB_2 with small amounts of MgO and un-reacted Mg and SiC. The unreacted Mg can be detected because of the high content of SiC in the raw materials.[11,12,18] The most interesting phase change relates to change in the Mg_2Si content with sintering temperature. 750in shows very high Mg_2Si content, which decreases with the sintering temperature and becomes a trace peak in 1050 in. However, more than a trace of Mg_2Si can only be found in 750inex and 850inex. The variation of Mg_2Si content is an important signal of the C and Si distribution in the MgB_2 matrix. Figure 2 shows the SEM images of 850in and 850inex. The 850in sample contains big-size slits between MgB_2 clusters as a result of the volume contraction during *in situ* sintering of Mg and B powders. The 850inex sample shows hard-packed MgB_2 clusters because the *ex situ* precursor is nucleating the center and releasing the strain of the *in situ* MgB_2.

The critical transition temperatures (T_c) of the two batches of samples are compared in Fig. 3. It is found that the T_c values of the *in situ*-sintered samples are always slightly lower than those for the samples from the other batch, except for 1050in, and the T_c dependence on sintering temperature of the two batches of samples is exactly the same, which means that the T_c depends greatly on the sintering temperature, but not on the different techniques. However, the

a)Electronic mail: shi@uow.edu.au.

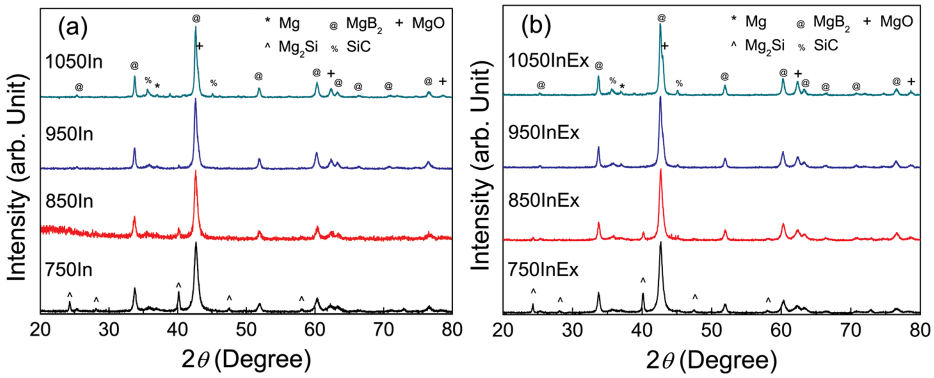

FIG. 1. (Color online) XRD patterns of nano-SiC doped MgB_2/Fe wires fabricated by (a) the *in situ* technique, and (b) the *in situ/ex situ* technique, with sintering at 750, 850, 950, and 1050 °C, respectively. All patterns were indexed with MgB_2, MgO, Mg_2Si, SiC, and Mg.

transition widths from the normal state to the superconducting state are quite different for the two batches of samples, as shown in the inset of Fig. 3. The transition widths of the *in situ* sintered samples are quite broad. The transition width is about 4 K for 750in and becomes 3 K in the 850in and 950in samples sintered at higher temperature because the high crystallinity. It should be noted that the transition of 1050in shows a two-step behavior, which may be attributed to the inhomogeneous carbon substitution effect or the inhomogeneous SiC distribution in the raw materials. The transition widths of all the samples made by the *in situ/ex situ* combined technique are 2.5 K. This means that the crystallinity is increased through the *in situ/ex situ* combined technique because the precursor MgB_2 powder is a source of high-quality nucleating centers for newly formed MgB_2 during the solid–liquid reaction between magnesium and boron.

The J_c dependence on the applied field is shown in Fig. 4 for typical samples, which were measured at 5 K and 20 K, respectively. It should be noted that the J_c dependence on sintering temperature in this work is totally different from previously reported results, because the solid–liquid reaction dynamics is different because of the small SiC particle size, less than 15 nm, which is much smaller than particle sizes used before. It is concluded that the *in situ/ex situ* combined technique only requires a lower sintering temperature to achieve high-quality MgB_2 wires, which is very important for industrial application in terms of the energy saving and equipment simplification. To avoid the influence of the flux jumping effect, the low-field performances were compared at 20 K in detail, as shown in the inset of Fig. 4. 750in and 750inex show quite low J_c values in lower magnetic field. 1050in and 850inex show competitive self-field J_c. The ball-milling process used to produce the *ex situ* MgB_2 powder destroyed the porous structure and enhanced the density of MgB_2 fabricated by the *in situ/ex situ* combined process. It is because of the small particle size of SiC used in this work, which induces different reaction dynamics during the *in situ* or *in situ/ex situ* processing,[2,12,16,17] that the present J_c dependence on sintering temperature is quite different from what has been previously reported. It is proposed that the liquid Mg reacts with SiC first to form Mg_2Si and release free C at low sintering temperature, and then the Mg_2Si reacts with B to form MgB_2 and release free Si at high sintering temperature. Both C and Si are very small and cannot be detected by XRD. The coherence length of MgB_2 is anisotropic. $\xi_{ab}(0) = 3.7–12$ nm, and $\xi_c(0) = 1.6 \sim 3.6$ nm,[19] which is shorter than the particle size of Mg_2Si. The Mg_2Si particles cannot be effective flux-pinning centers, but are useless impurities in the MgB_2 matrix, which decrease the density of current carriers. However, the free C and Si can be very strong flux-pinning centers because of their small sizes, which is responsible for the high J_c performance in high magnetic fields. According to the collective pinning model,[21] the density of current carriers is responsible for the J_c performance in the single-vortex pinning regime because of its weak field dependence, while the flux-pinning force is responsible for the J_c performance in the small-bundle regime because of the increased high H_{c2} and H_{irr}. The approximate H_{sb} values are also indicated on the J_c curves estimated at 20 K, as shown in the inset of Fig. 4, where H_{sb} is the crossover field from single-vortex to small-bundle

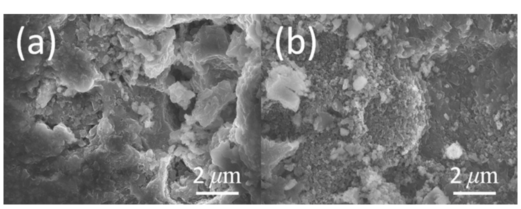

FIG. 2. SEM photos of (a) 850in, and (b) 850inex.

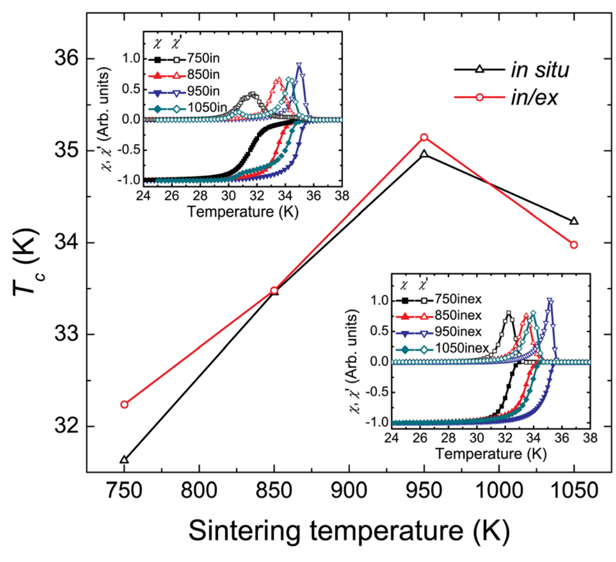

FIG. 3. (Color online) Comparison of the dependence of the critical transition temperature T_c on sintering temperature. The insets show the normalized magnetic moment dependence on temperature for all *in situ* samples (upper) and for all *in situ/ex situ* samples (lower).

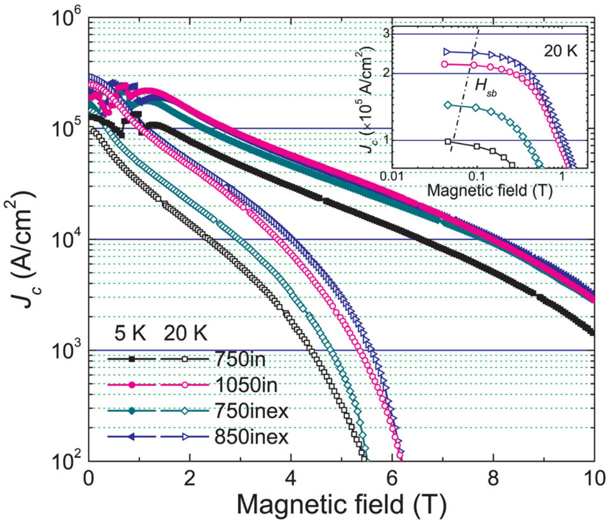

FIG. 4. (Color online) The dependence of critical current density, J_c, on applied magnetic field at 5 K and 20 K for typical samples. The inset shows the J_c performance in low magnetic field at 20 K. H_{sb}, the crossover field from single-vortex to small-bundle pinning, is indicated by the dashed-dotted line.

pinning. However, H_{sb} has not been detected at 5 K because of the relatively high supercurrents.[22]

The strength of the pinning force can be reflected by the dependence of H_{c2} and H_{irr} on normalized temperature, as shown in Fig. 5. Carbon substitution is one of the most effective methods to improve the H_{c2} and H_{irr} because of the increased scattering by C doping, and the increased scattering can also contribute to decreased T_c and merging of the two gaps.[20] It should be noted that the H_{c2} and H_{irr} for 750in, 850in, and 750inex are highest at low temperature, which means a strong flux-pinning force. Their poor J_c is attributed to the lower density of current carriers. Both 1050in and 1050inex show the lowest H_{c2} and the lowest H_{irr} among all the samples. 850in, 950in, 850inex, and 950inex show competitive H_{c2} and H_{irr} performances, which are responsible for their high J_c values under high magnetic field.

In conclusion, high sintering temperature can improve the critical current density of small-particle size SiC-doped MgB_2. The two-step reactions between Mg, SiC, and B release free C and Si to form strong flux-pinning centers. The current carrier density and flux-pinning force are important factors in improvement of the J_c performance of nano-SiC-doped MgB_2.

The authors thank Dr. T. Silver for her useful discussions. This work is supported by the Australian Research Council (project ID: DP0770205) and Hyper Tech Research Inc.

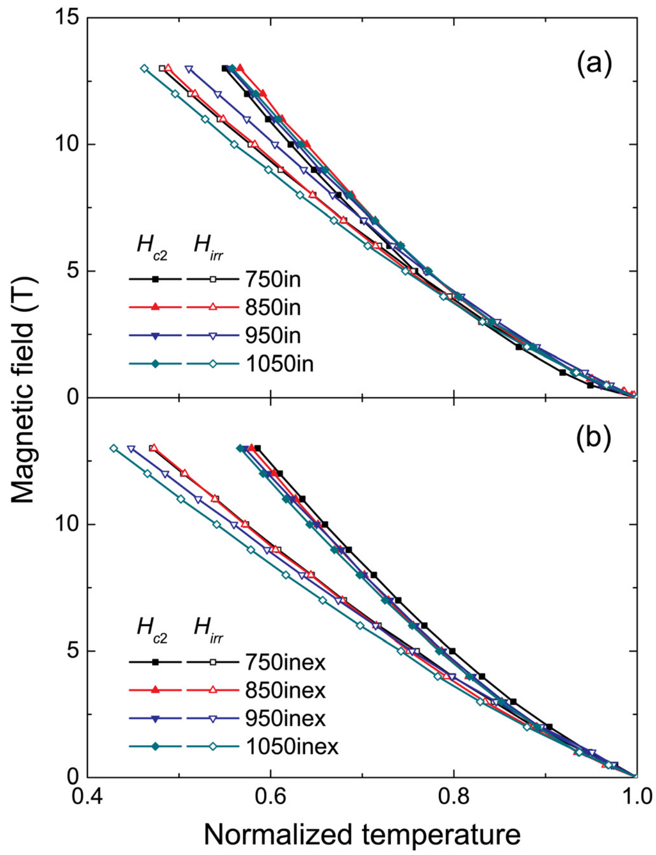

FIG. 5. (Color online) Comparison of H_{c2} (solid symbols) and H_{irr} (open symbols) for (a) *in situ* MgB_2/Fe wires doped with nano-SiC, and (b) *in situ*/*ex situ* MgB_2/Fe wires doped with nano-SiC.

[1] E. W. Collings, M. D. Sumption, M. Bhatia, M. A. Susner, and S. D. Bohnenstiehl, Supercond. Sci. Technol. **21**, 103001 (2008).
[2] S. X. Dou, S. Soltanian, J. Horvat, X. L. Wang, S. H. Zhou, M. Ionescu, H. K. Liu, P. Munroe, and M. Tomsic, Appl. Phys. Lett. **81**, 3419 (2002).
[3] S. X. Dou, W. K. Yeoh, J. Horvat, and M. Ionescu, Appl. Phys. Lett. **83**, 4996 (2003).
[4] W. X. Li, Y. Li, R. H. Chen, W. K. Yeoh, and S. X. Dou, Physica C **460**, 570 (2007).
[5] W. K. Yeoh, J. Horvat, S. X. Dou, and P. Munroe, IEEE Trans. Appl. Supercond. **15**, 3284 (2005).
[6] W. X. Li, Y. Li, M. Y. Zhu, R. H. Chen, X. Xu, W. K. Yeoh, J. H. Kim, and S. X. Dou, IEEE Trans. Appl. Supercond. **17**, 2778 (2007).
[7] R. H. Chen, M. Y. Zhu, Y. Li, W. X. Li, H. M. Jin, and S. X. Dou, Acta Phys. Sin. **55**, 4878 (2006).
[8] X. P. Zhang, Y. W. Ma, Z. S. Gao, Z. G. Yu, K. Watanabe, and H. H. Wen, Acta Phys. Sin. **55**, 4873 (2006).
[9] C. G. Zhuang, S. Meng, C. Y. Zhang, Q. R. Feng, Z. Z. Gan, H. Yang, Y. Jia, H. H. Wen, and X. X. Xi, J. Appl. Phys. **104**, 013924 (2008).
[10] X. H. Zeng, A. V. Pogrebnyakov, M. H. Zhu, J. E. Jones, X. X. Xi, S. Y. Xu, E. Wertz, Q. Li, J. M. Redwing, J. Lettieri, V. Vaithyanathan, D. G. Schlom, Z. K. Liu, O. Trithaveesak, and J. Schubert, Appl. Phys. Lett. **82**, 2097 (2003).
[11] W. X. Li, Y. Li, R. H. Chen, R. Zeng, S. X. Dou, M. Y. Zhu, and H. M. Jin, Phys. Rev. B **77**, 094517 (2008).
[12] W. X. Li, R. Zeng, L. Lu, Y. Li, and S. X. Dou, J. Appl. Phys. **106**, 093906 (2009).
[13] W. X. Li, R. Zeng, Y. Zhang, X. Xu, Y. Li, and S. X. Dou, IEEE Trans. Appl. Supercond. **21**, 2635 (2011).
[14] A. Serquis, L. Civale, D. L. Hammon, X. Z. Liao, J. Y. Coulter, Y. T. Zhu, M. Jaime, D. E. Peterson, F. M. Mueller, V. F. Nesterenko, and Y. Gu, Appl. Phys. Lett. **82**, 2847 (2003).
[15] W. X. Li, R. H. Chen, Y. Li, M. Y. Zhu, H. M. Jin, R. Zeng, S. X. Dou, and B. Lu, J. Appl. Phys. **103**, 013511 (2008).
[16] S. X. Dou, A. V. Pan, S. Zhou, M. Ionescu, X. L. Wang, J. Horvat, H. K. Liu, and P. R. Munroe, J. Appl. Phys. **94**, 1850 (2003).
[17] S. X. Dou, A. V. Pan, S. Zhou, M. Ionescu, H. K. Liu, and P. R. Munroe, Supercond. Sci. Technol. **15**, 1587 (2002).
[18] Y. Zhang, S. X. Dou, C. Lu, H. Zhou, and W. X. Li, Phys. Rev. B **81**, 094501 (2010).
[19] C. Buzea and T. Yamashita, Supercond. Sci. Technol. **14**, R115 (2001).
[20] M. Angst, S. L. Bud'ko, R. H. T. Wilke, and P. C. Canfield, Phys. Rev. B **71**, 144512 (2005).
[21] G. Blatter, M. V. Feigelman, V. B. Geshkenbein, A. I. Larkin, and V. M. Vinokur, Rev. Mod. Phys. **66**, 1125 (1994).
[22] W. X. Li, R. Zeng, L. Lu, and S. X. Dou, J. Appl. Phys. **109**, 07E108 (2011).